British Journal of Pharmacology

DOI:10.1111/j.1476-5381.2012.02120.x
www.brjpharmacol.org

RESEARCH PAPER

Activation of PAR_2 receptors sensitizes primary afferents and causes leukocyte rolling and adherence in the rat knee joint

FA Russell[1], N Schuelert[1], VE Veldhoen[1], MD Hollenberg[1] and JJ McDougall[2]

[1]*Department of Physiology & Pharmacology, University of Calgary, Calgary, AB, Canada, and*
[2]*Departments of Pharmacology and Anaesthesia, Dalhousie University, Halifax, NS, Canada*

Correspondence
Dr Jason J McDougall, Departments of Pharmacology and Anaesthesia, Dalhousie University, 5850, College Street, Halifax, NS, Canada B3H 4R2.
E-mail: jason.mcdougall@dal.ca

Keywords
PAR_2; joint pain; inflammation; leukocyte accumulation

Received
23 January 2012
Revised
8 May 2012
Accepted
29 May 2012

BACKGROUND AND PURPOSE

The PAR_2 receptors are involved in chronic arthritis by mechanisms that are as yet unclear. Here, we examined PAR_2 activation in the rat knee joint.

EXPERIMENTAL APPROACH

PAR_2 in rat knee joint dorsal root ganglia (DRG) cells at L3-L5, retrogradely labelled with Fluoro-gold (FG) were demonstrated immunohistochemically. Electrophysiological recordings from knee joint nerve fibres in urethane anaesthetized Wistar rats assessed the effects of stimulating joint PAR_2 with its activating peptide, 2-furoyl-LIGRLO-NH_2 (1–100 nmol·100 μL^{-1}, via close intra-arterial injection). Fibre firing rate was recorded during joint rotations before and 15 min after administration of PAR_2 activating peptide or control peptide. Leukocyte kinetics in the synovial vasculature upon PAR_2 activation were followed by intravital microscopy for 60 min after perfusion of 2-furoyl-LIGRLO-NH_2 or control peptide. Roles for transient receptor potential vanilloid-1 (TRPV1) or neurokinin-1 (NK_1) receptors in the PAR_2 responses were assessed using the selective antagonists, SB366791 and RP67580 respectively.

KEY RESULTS

PAR_2 were expressed in 59 ± 5% of FG-positive DRG cells; 100 nmol 2-furoyl-LIGRLO-NH_2 increased joint fibre firing rate during normal and noxious rotation, maximal at 3 min (normal; 110 ± 43%, noxious; 90 ± 31%). 2-Furoyl-LIGRLO-NH_2 also significantly increased leukocyte rolling and adhesion over 60 min. All these effects were blocked by pre-treatment with SB366791 and RP67580 ($P < 0.05$ compared with 2-furoyl-LIGRLO-NH_2 alone).

CONCLUSIONS AND IMPLICATIONS

PAR_2 receptors play an acute inflammatory role in the knee joint via TRPV1- and NK_1-dependent mechanisms involving both PAR_2-mediated neuronal sensitization and leukocyte trafficking.

Abbreviations

DRG, dorsal root ganglia; NK_1, neurokinin 1; TRPA1, transient receptor potential ankyrin receptor 1; TRPV1, transient receptor potential vanilloid receptor 1

Introduction

The GPCR family of proteinase-activated receptors ($PAR_{1,2,3,4}$: receptor nomenclature follows Alexander *et al.*, 2011) are unique in their mechanism of activation. Instead of responding to a soluble ligand, PARs are activated by the binding of a ligand within their amino-terminal extracellular domain. This 'tethered ligand' is only able to bind to the extracellular

receptor activation domain after it has been unmasked by proteolytic cleavage at a specific extracellular N-terminal site on the receptor (Hollenberg and Compton, 2002; Adams *et al.*, 2011). All four PARs are targeted by various serine proteinases including thrombin, trypsin, tissue kallikrein-14 (KLK14) and tryptase that can normally act on more than one of the PARs (Russell and McDougall, 2009; Adams *et al.*, 2011). PAR_2 was the second PAR to be identified and, unlike the other three members, is not activated by thrombin, but is preferentially activated by trypsin, KLK14 and other serine proteinases (Macfarlane *et al.*, 2001; Oikonomopoulou *et al.*, 2006). In the laboratory setting, receptor-selective synthetic receptor-activating peptides that mimic the tethered ligand for each PAR have been developed, thus allowing studies of PAR activation without the need for receptor proteolysis. Using these synthetic PAR-activating peptides and mouse knock-out models, PAR_2 and its activating proteinases have been shown to play important pro-inflammatory and pro-nociceptive roles in the joint and other tissues (Steinhoff *et al.*, 2000; Ferrell *et al.*, 2003; Hansen *et al.*, 2005; Kelso *et al.*, 2006; Ramachandran and Hollenberg, 2008; Russell and McDougall, 2009; Helyes *et al.*, 2010). PAR_2 activating peptides cause oedema, leukocyte accumulation and hyperalgesia when injected into the rodent hind paw (Vergnolle *et al.*, 1999; 2001; Kawabata *et al.*, 2001) and promote visceral hyperalgesia in the colon (Coelho *et al.*, 2002). The hind paw is a useful model in which to observe acute peripheral inflammation; however, the relevance of this model to human arthritic disease is not clear. Given the substantial clinical importance of arthritis, it is imperative to study the mechanisms underlying joint inflammation in order to understand how this disease progresses and to develop improved treatments for this illness. PAR_2 knock-out mice exhibit significantly less joint swelling and damage in chronic models of joint inflammation (Ferrell *et al.*, 2003; Yang *et al.*, 2005; Busso *et al.*, 2007). Recently, it has been shown that intra-articular injections of the PAR_2-activating peptide, SLIGRL-NH_2, causes swelling, cytokine release and increased sensitivity to pain in the mouse knee joint (Helyes *et al.*, 2010). Therefore, it is clear that, as in the hind-paw, PAR_2 receptors have a role in joint inflammation and pain. The mechanisms underlying this role of PAR_2 in the joint are just beginning to be elucidated. There is evidence that PAR_2 receptors and the transient receptor potential vanilloid 1 (TRPV1) ion channels are co-expressed in dorsal root ganglia (DRG) neurones, suggesting a link between these two receptor systems (Amadesi *et al.*, 2004). Indeed, the secondary mechanical allodynia and change in weight distribution induced by intra-articular SLIGRL-NH_2 were shown to be TRPV1-dependent (Helyes *et al.*, 2010). This observation correlates with data obtained in other tissues, such as the paw where PAR_2 agonists induce hyperalgesia, dependent on both TRPV1 channels and the substance P receptor, NK_1 (Vergnolle *et al.*, 2001; Amadesi *et al.*, 2004). Furthermore, in the skin, inflammation induced by the proteinases, trypsin and tryptase is mediated via PAR_2 activation and the subsequent TRPV1-dependent release of the neuropeptides, substance P and calcitonin gene-related peptide (CGRP), leading to neurogenic inflammation (Steinhoff *et al.*, 2000; Costa *et al.*, 2008). In contrast, the increase in IL-1β seen in the joint after PAR_2 activation was TRPV1-independent (Helyes *et al.*, 2010). Importantly, PAR_2 agonists can activate non-TRPV1-expressing DRG neurons (Alier *et al.*, 2008), suggesting that there are both TRPV1-dependent and -independent effects of PAR_2.

Given the lack of mechanistic information about the effects of PAR_2 activation on joint pathophysiology, our aim was to characterize further the inflammatory and neuronal events that occur in the knee joint upon PAR_2 activation. To this end, we first verified the presence of PAR_2 in articular sensory neurones, using an immuno-gold/immunohistochemical approach, and then used an improved potent receptor-selective PAR_2-activating peptide (2-furoyl-LIGRLO-NH_2) (Kawabata *et al.*, 2004; Hollenberg *et al.*, 2008) to activate PAR_2 in the joint. This agonist acts at lower concentrations than the one we had previously used (SLIGRL-NH_2) and is therefore better adapted for studies targeting the joint. The effects of intra-articular administration of the PAR_2-activating peptide were monitored both with real-time *in vivo* electrophysiological recordings of afferent neuronal activity and with intravital microscopy to evaluate changes in the joint microvasculature. In addition, using selective receptor antagonists, we investigated the role of TRPV1 and NK_1 receptors in the PAR_2-induced responses. We determined that PAR_2 activation leads to neuronal and inflammatory changes in the joint that are reliant on TRPV1 and NK_1 receptor-dependent mechanisms.

Methods

Test systems used

All animal handling and experimental procedures outlined in this study were in accordance with the Canadian Council for Animal Care guidelines for the care and use of experimental animals and all protocols used were approved by the University of Calgary Health and Sciences Animal Care Committee. The studies involving animals are reported in accordance with the ARRIVE guidelines for reporting experiments involving animals (McGrath *et al.*, 2010).

Expression, electrophysiology and intravital experiments were used male Wistar rats (n = 72, 250–450 g; Charles River Laboratories, Quebec, Canada). Additional electrophysiological experiments to confirm the specificity of the PAR_2 activating peptide were performed on male PAR_2 wild-type (WT) and PAR_2 null (KO) mice (n = 10, 25–35 g, developed on a C57Bl6 background, a gift from Johnson & Johnson Pharmaceutical Research & Development, Spring House, PA, USA) (Damiano *et al.*, 1999). Mice were only used in this one experiment due to technical limitations. In order to study the effect of repeated drug administrations and antagonists on single nerve fibres, it was necessary to use Wistar rats as the model system for all further experiments. All animals were housed in a climatically controlled environment with a regular 12 h dark/light cycle and with access to food and water *ad libitum*.

Fluoro-gold labelling of knee joint afferents

Knee joint afferents were labelled using the retrograde fluorescent dye, Fluoro-Gold, as described previously (Russell *et al.*, 2010). Four naive rats were anaesthetised with 2% isoflurane. The knee was shaved and placed in a holder so that the angle between patella and femur was approximately 45°.

The patellar ligament was exposed by making a 3–4 mm longitudinal incision in the skin. Using a 30G needle, a Hamilton syringe and a micromanipulator, 10 µL of Fluoro-Gold (2% solution in saline; Fluorochrome, Denver, CO, USA) was injected into the space between the patella and groove of the distal femur. The knee was flexed and extended for 30 s, and 15 µL of a 0.2 M PBS solution was then injected. After needle withdrawal, the wound was sealed with skin glue. This procedure was repeated on the contralateral knee, and the rat was allowed to recover for 4 days. The cell bodies of rat knee joint afferents are known to be contained within L3–L5 DRGs (Salo and Theriault, 1997). Thus, after 4 days, the rats were killed with euthanyl (sodium pentobarbital 240 $mg \cdot mL^{-1}$; Bimdea, Animal Health Inc, Ontario, Canada); and bilateral DRGs from L3, L4 and L5 were removed and fixed in 4% paraformaldehyde (PFA) overnight. Following fixation, the DRGs were placed in 30% sucrose solution at 4°C overnight, then embedded in OCT (Sakura Finetek, Torrance, CA, USA) and frozen at –80°C until sectioning. DRG sections were cut at 12 µm and mounted on Superfrost Plus slides (Fischer Scientific, Nepean, Ottawa, Canada) with each slide containing 10–12 consecutive sections from the DRG. This approach allowed for a comparison between consecutive sections so that Fluoro-Gold positive cells were counted once only.

Fluorescence immunohistochemistry

DRG sections were treated for 10 min with 0.2% Triton-X/PBS then washed 3 × 5 min in 0.2% Tween 20/PBS. Sections were then blocked with 10% normal goat serum for 1 h at room temperature and incubated overnight at 4°C with polyclonal A5 rabbit anti-PAR_2 antibody targeted to the cleavage–activation sequence in the receptor, developed as previously described for the B5 antiserum (Al-Ani *et al.*, 1999) (dilution, 1:250). Slides were washed 2 × 5 min with 0.2% Tween 20/PBS, and specific PAR_2 staining was then detected by incubating slides for 1 h at room temperature with a Cy3-labelled goat anti-rabbit IgG (1:500, Jackson Immunoresearch Laboratories, West Grove, PA, USA). Slides were washed for a final 2 × 5 min with 0.2% Tween 20/PBS in the dark and coverslipped with ProLong Gold Anti-fade (Invitrogen, Burlington, Ontario, Canada). Imaging was analysed using Open Lab 3.0 software (Quorum Technologies Inc., Guelph, Ontario, Canada) on a Leica DM6000B fluorescence microscope (Leica, Wetzlar, Germany). A cell was deemed positive for PAR_2 when labelling showed an obvious outline of the cell and the nucleus was clearly visible. Specificity of the PAR_2 primary antibody was determined both through omission of the primary antibody and by pre-incubating the primary antibody with a blocking immunizing peptide (GPNSKGRSLIGRLDTP: 20 $\mu g \cdot mL^{-1}$) for 2 h before staining. No staining was observed under either of these conditions (data not shown). Every DRG section was examined under appropriate filters for Fluoro-Gold (A cube, Leica Microsystems with excitation: 340–380 nm, long-pass emission filter: 425 nm) and Cy3 (excitation: 550 nm, emission 570 nm). The diameter of all Fluoro-Gold positive cells was measured, and the size distribution of Fluoro-Gold positive cells was found to correspond with previous reports of DRG labelled joint neurons (Ivanavicius *et al.*, 2004; Russell *et al.*, 2010). No Fluoro-Gold labelling was seen in DRG sections from rats that were not injected with Fluoro-Gold (data not shown).

Surgical procedures

Deep anaesthesia was achieved in both rats and mice using urethane (25% stock solution; 2 $g \cdot kg^{-1}$ i.p.) and was confirmed by the absence of the hind paw withdrawal reflex before any surgical procedures were performed. Rats were artificially ventilated by a Harvard rodent respiratory pump (Harvard Apparatus, Holliston, MA, USA) with 100% O_2 (stroke volume of 2.5 mL, breath frequency set at 60 $breaths \cdot min^{-1}$), after cannulation of the trachea. A fine-bore catheter [0.5 mm inner diameter (ID), 1.00 mm outer diameter (OD); Portex, Kent, UK] containing heparinized saline (100 $units \cdot mL^{-1}$) was used to cannulate the left carotid artery. This cannula enabled connection to a pressure transducer to allow for continuous blood pressure measurement with a blood pressure monitor (BP-1; World Precision Instruments, Sarasota, FL, USA). The left jugular vein was also cannulated (fine-bore tubing, 0.40 mm ID, 0.80 mm OD; Portex) to permit injection of the muscle relaxant gallamine triethiodide (50 $mg \cdot kg^{-1}$) to eliminate neural interference from the hind limb musculature. Core body temperature was measured using a rectally inserted thermometer and maintained at 37°C by a thermostatically controlled heating blanket.

To immobilize the proximal aspect of the rat hind limb, a specialized clamp fixed to a stereotaxic frame was attached to the isolated mid portion of the right femur bone. An incision in the skin was made longitudinally along the medial aspect of the hind limb, and the right saphenous artery was cannulated (fine-bore tubing, 0.28 mm ID, 0.61 mm OD; Portex) with the tubing placed below the knee joint and advanced to a point just distal to the bifurcation with the medial articular artery. This positioning permitted the local intra-arterial injection of drugs directly to the joint. Skin flaps from the hind limb were sutured to a metal O-ring and the consequent pouch that these sutures created was filled with warm paraffin oil (37°C) to prevent tissue desiccation. The right hind-paw was held in a shoe-like holder connected to a force transducer and torque meter (Data Track 244-1-R, Intertechnology Inc., Toronto, Ontario, Canada). This arrangement enabled standardization of the amount of rotational force being applied to the knee joint.

Deep anaesthesia was achieved in mice using urethane (25% stock solution; 2 $g \cdot kg^{-1}$ i.p.) and was confirmed by the absence of the hind paw withdrawal reflex before any surgical procedures were done. Mice were artificially ventilated by a Harvard rodent respiratory pump (Harvard Apparatus) with 100% O_2 (stroke volume of 0.25 mL, breath frequency set at 150 $breaths \cdot min^{-1}$). The muscle relaxant gallamine triethiodide (50 $mg \cdot kg^{-1}$) was injected into the jugular vein to eliminate neural interference from the hind limb musculature. An incision in the skin was made longitudinally along the medial aspect of the hind limb. Skin flaps from the hind limb were sutured to a metal O-ring and the consequent pouch that these sutures created was filled with warm paraffin oil (37°C) to prevent tissue desiccation.

Extracellular electrophysiological recording

The technique used for recording rat knee joint afferent nerve fibres has been described previously (Russell *et al.*, 2010). Briefly, the saphenous nerve was transected distally to the knee joint in order to eliminate sensory input from the foot and ankle region. The nerve was then isolated in the inguinal

region of the hind limb and cut centrally to block the generation of spinally mediated reflexes. A small, black Perspex stage was placed in the oil pool to assist the visualization of the remaining saphenous nerve stump projecting from the knee. Placement of the nerve stump on this black stage facilitated the isolation of neurofilaments. The epineurium was removed from a small section of the nerve, and fine watchmaker forceps were utilized to dissect fine neurofilaments free from the nerve. These small neurofilaments were then placed over a platinum electrode to permit extracellular recordings. Only afferent nerve fibres originating from the knee joint were recorded from and these were identified by a firing response elicited by gentle probing of the knee joint using a glass rod with a 1-mm tip.

The electrical threshold of each joint fibre was determined by placing a pair of bipolar silver wire electrodes (1 Hz, 100 ms pulse width) in the receptive field of the fibre and gradually increasing the voltage of stimulation in 0.5V steps until the pulse elicited spike discharges from the afferent nerve. To determine the conduction velocity of the nerve fibres, the distance between stimulating and recording electrodes was divided by the latency between stimulus artefact and evoked afferent impulse. In approximately 25% of fibres, it was impossible to determine the conduction velocity as the units were not activated by electrical stimulation, possibly due to them having a deep receptive field. The mechanical threshold of each fibre was revealed by slowly rotating the knee and noting the lowest force, as measured with the torque meter, that elicited nerve activity.

Four movement cycles, each consisting of 10 s of normal non-noxious rotation and 10 s of noxious hyper-rotation of the knee to discrete torque levels, were performed at the beginning of the experiment. Normal rotation is defined here as movement occurring within the normal working range of the joint, which would be perceived as a non-noxious stimulus. In contrast, noxious hyper-rotation of the joint is defined as movement occurring outside the normal working range of the knee without leading to serious tissue damage. This level of joint rotation causes high frequency firing of joint primary afferent nerve fibres, which would be interpreted as a painful sensation in an awake animal.

The mean afferent nerve fibre firing rate associated with these four movements was the control baseline level. Then, either the PAR_2 activating peptide, 2-furoyl-LIGRLO-NH_2 (at doses 1, 10 and 100 nmol in 100 μL) or the inactive scrambled control peptide, 2-furoyl-OLGRIL-NH_2 (100 nmol·100 μL^{-1}) was administered via the saphenous arterial cannulation. This route of administration was favoured over an intra-articular injection approach so as to reduce the risk of damage to the primary afferent nerve ending and to allow multiple doses of drug to be administered to each fibre. Movement cycles were repeated 1 min after drug administration and then every 2 min until 15 min after drug. Rats were either naive or pretreated with the TRPV1 antagonist, SB366791 (500 $\mu g \cdot kg^{-1}$ i.p. 30 min before administration of the PAR_2 agents) (Helyes *et al.*, 2010). In a separate group of animals, the NK_1 receptor antagonist, RP67580 (2 nmol) (McDougall *et al.*, 2001), was administered either alone via the saphenous cannulation or co-administered together with 100 nmol 2-furoyl-LIGRLO-NH_2. Previous experiments have validated these routes of administration for effective blockade of NK_1 and TRPV1 receptors with their respective antagonists (McDougall *et al.*, 2001; Helyes *et al.*, 2010).

Neuronal activity was digitized using a data acquisition system (CED1401; Cambridge Electronic Design, Cambridge, UK) and stored on a microcomputer for offline analysis. The number of action potentials (APs) per movement was determined using Spike 2 software (Cambridge Electronic Design), and the percentage change in afferent nerve fibre activity from baseline was calculated.

In mice, the nerve dissection and identification of joint afferents was done the same way as for the rat experiments as described above. However, instead of a single unit, multiple units were identified and recorded as a sum action potential. After identification of multiple units as joint afferents without muscle input. a cannulation tube (fine-bore tubing, 0.40 mm ID, 0.80 mm OD; Portex) was filled with 20 μL of 2-furoyl-LIGRLO-NH_2 (100 nmol in 100 μL) and 20 μL of KCl solution (0.4 mM). Both solutions were separated by a small air bubble in the tube. The tube was connected to a Hamilton syringe. A 30G needle was inserted into the tube and then inserted into the space between the patella and groove of the distal femur. After confirming that the recorded units have not been damaged by the inserted needle and still respond to probing of the receptive field, first 2-furoyl-LIGRLO-NH_2 was injected intra-articular. and nerve activity was recorded for 15 min. For analysis, the sum action potential of all afferents was determined before and 15 min after injection of 2-furoyl-LIGRLO-NH_2 by calculating the number of action potentials elicited in a 1 min timeframe. Then KCl was injected to confirm that the injected drug reached the joint nerve terminals in all experiments.

Intravital microscopy of the synovial microcirculation

Rats were deeply anaesthetized as mentioned previously. The skin and connective tissue over the right knee were surgically removed to expose the antero-medial aspect of the knee joint, and animals were placed in dorsal recumbency on a homoeothermic heating blanket. The exposed knee joint was immediately and continuously perfused with warm (37°C) 0.9% saline at a rate of 12 $mL \cdot h^{-1}$ using a peristaltic pump (Gilson, Guelph, Ontario, Canada) and secured in a presentation suitable for microscopy. A glass coverslip was gently placed over the medial aspect of the knee joint and secured to the stage with vacuum grease.

Leukocytes were stained *in vivo* by i.v. injection of 0.05% Rhodamine 6G (Sigma-Aldrich) through a tail vein cannulation. The microcirculation was examined under incident fluorescent light microscopy using a Mikron IV 500 microscope (Mikron Instruments, San Marcos, CA, USA) with a ×40 objective lens (Zeiss Achroplan 40X/0.75W) and a Periplan ×10 eyepiece (final magnification ×400). Straight, unbranched, post-capillary venules (diameter 20–50 μm), located directly on the knee joint capsule, were selected for analysis. Leukocyte kinetics was recorded using a XR/MEGA-10 video camera (Stanford Photonics, Palo Alto, CA, USA). A 1 min control recording was acquired before any drug perfusion. Then either the PAR_2 activating peptide, 2-furoyl-LIGRLO-NH_2 (at 1, 10 and 1000 μM) or the PAR_2-inactive scrambled control peptide, 2-furoyl-OLGRIL-NH_2 (1000 μM) were perfused over the knee joint for 5 min. After this time, warm

saline (37°C) was continuously perfused; and 1 min recordings made at 5, 10, 20, 30, 40, 50 and 60 min after drug perfusion. Rats were either naive or pre-treated with the TRPV1 antagonist, SB366791 (500 $\mu g \cdot kg^{-1}$ i.p. 30 min before administration of the PAR_2 agents). In a separate group of animals, the NK_1 antagonist, RP67580 (2 nmol), was co-perfused together with 2-furoyl-LIGRLO-NH_2. Recordings were also made during saline perfusion alone on another group of animals. Recordings were subsequently analysed offline to determine leukocyte trafficking within the microvasculature. Leukocyte kinetics in the joint were defined as described previously (Andruski *et al.*, 2008). Briefly, a rolling leukocyte is defined as a white blood cell moving slower than the normal flow of blood in a given vessel. The extent of leukocyte rolling is expressed as leukocyte flux and calculated as the number of rolling cells to pass an arbitrarily defined line perpendicular to the axis of the vessel in 1 min. A leukocyte is classified as adherent if it remains stationary for at least 30 s, and total leukocyte adhesion was quantified as the number of adherent cells within a 100 µm length of venule in 1 min.

Data analysis and statistical procedures

All data were normally distributed and were therefore tested using parametric statistics. Data were expressed as means ± SEM. To analyse different drug treatments and time effects between experimental groups two-way ANOVA and Bonferroni post tests were used; $P < 0.05$ was considered statistically significant. Time courses of drug effects were analysed using a repeated-measures one-way ANOVA with individual time points compared against baseline using the Dunnett's multiple comparison test.

Materials

The PAR_2-activating peptide, 2-furoyl-LIGRLO-NH_2, the PAR_2-inactive scrambled control peptide, 2-furoyl-OLGRIL-NH_2, were obtained from the Peptide Synthesis Facility at the University of Calgary (peplab@ucalgary.ca, Calgary, Alberta, Canada). The composition and purity of the peptides were confirmed by HPLC and mass spectral analysis. All peptides were dissolved in sterile 0.9% NaCl. SB366791 (Sigma-Aldrich, Ontario, Canada) was dissolved in 2% DMSO and 1% cremophor. RP67580 (Tocris Bioscience, Missouri, MO, USA) was dissolved in 1% ethanol. The polyclonal A5 rabbit anti-PAR_2 antiserum was prepared using a synthetic immunizing peptide containing the PAR_2-derived sequence: G_3PNSKGRSLIGRLDTP as described previously (Al-Ani *et al.*, 1999); this synthetic peptide, also synthesised by the University of Calgary peptide synthesis facility, was used at a concentration of 20 $\mu g \cdot mL^{-1}$ to block the reaction of the A5 antiserum with the tissue PAR_2 epitope.

Results

Fluoro-gold labelling of knee joint afferents and co-localization of PAR_2 receptors

The initial objective of this study was to verify the co-localization of PAR_2 receptors on the cell bodies of rat knee joint afferents that are found within the L3, L4 and L5 DRGs (Salo and Theriault, 1997) A total of 3436 Fluoro-gold positive neurones were identified in L3, L4 and L5 DRGs collected from four rats. On average 430 ± 48 labelled afferents were seen per injected knee joint and were seen to be of similar size distribution as observed in previous reports (Salo and Theriault, 1997; Russell *et al.*, 2010). The majority of joint afferents were observed in L3 and L4 DRGs (Table 1). Of the Fluoro-gold-positive cells, 59 ± 5% also stained positively for PAR_2. Photomicrographs from L3, L4 and L5 DRGs showing typical co-localization of Fluoro-gold and PAR_2 are shown in Figure 1. PAR_2 exhibited similar expression distribution in joint afferents associated with L3, L4 and L5 DRGs. In addition, no preferential expression in a particular size of neurone was observed as the distribution of Fluoro-gold- and PAR_2-positive cells corresponded to the overall size distribution of all Fluoro-gold-positive cells (Figure 2). Thus, a substantial proportion of the cell bodies with an afferent connection to the knee joint expressed PAR_2.

Table 1

Counts of Fluoro-Gold-positive cells and PAR_2-positive cells in L3, L4 and L5 DRGs

DRG	No. of Fluoro-Gold positive cells	No. of Fluoro-Gold cells positive for PAR_2	% of Fluoro-Gold cells positive for PAR_2
L3	263 ± 14	146 ± 19	56 ± 7
L4	206 ± 24	113 ± 9	58 ± 6
L5	48 ± 6	31 ± 5	62 ± 6

Values are mean ± SEM, $n = 8$.

Specificity of PAR_2-activating peptide

The specificity of the PAR_2 activating peptide, 2-furoyl-LIGRLO-NH_2, for triggering PAR_2 receptors was confirmed (i) by monitoring a lack of response to the receptor-inactive 'scrambled' peptide, 2-furoyl-OLRGIL-NH_2 (see below) and (ii) by conducting electrophysiological experiments comparing the responses of the PAR_2-activating peptide, 2-furoyl-LIGRLO-NH_2 observed in wild-type compared with PAR_2 knock-out mice. Intra-articular injection of 2-furoyl-LIGRLO-NH_2 in wild-type mice ($n = 6$) induced long-lasting spontaneous activity, starting 5 to 10 min after drug application in all recorded nerve afferents (Figure 3A). 15 min after drug administration the firing rate was significantly increased (1.7–8.9 Hz;) compared with control (0.0–to 0.36 Hz Figure 3C; $P < 0.01$; Student *t*-test). In PAR_2 knock-out mice ($n = 4$), 2-furoyl-LIGRLO-NH_2 had no effect on spontaneous activity in any of the recorded nerve afferents during the 15 min recording period (Figure 3D), thereby confirming its selectivity for activating PAR_2. Fifteen minutes after drug application, no significant changes in firing rate (0.05–0.35 Hz;) were observed compared with control (0.06–0.4 Hz; $P = 0.62$, Student *t*-test; Figure 3F). In all experiments, intra-articular injection of KCL induced a burst of activity that was quick in onset confirming that test reagents reached the nerve terminals in all recorded fibres (Figure 3B and E).

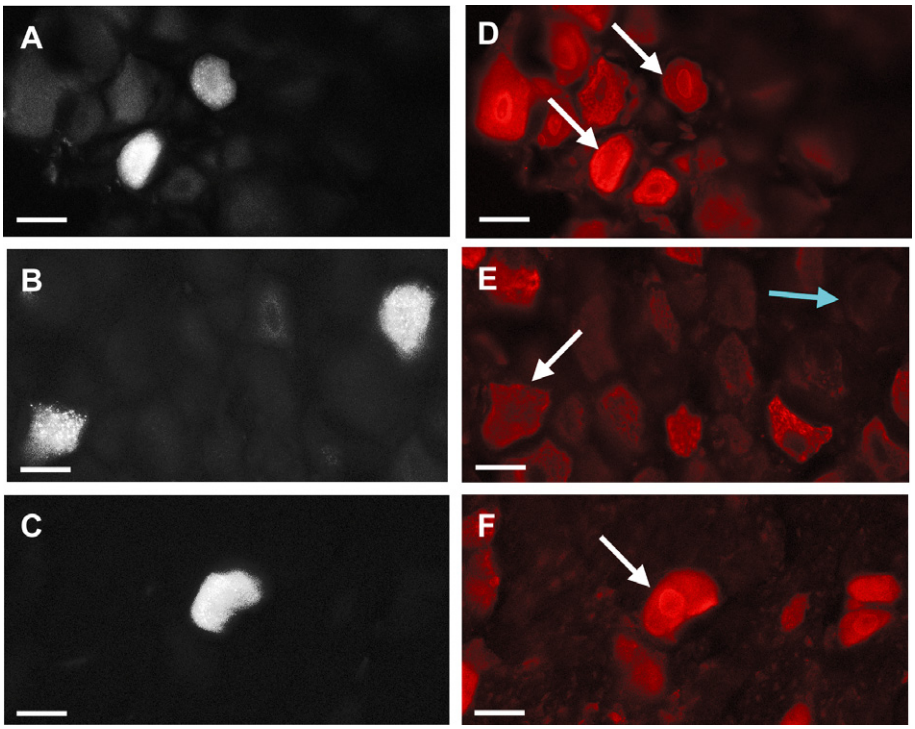

Figure 1

PAR_2 expression in knee joint afferent neuronal cell bodies. Left: Retrograde labelling of knee joint afferent DRGs with Fluoro-Gold taken from L3 (A), L4 (B) and L5 (C). Right: Immunofluorescent imaging using Cy3 reveals a co-localization of PAR_2-positive cells in the corresponding L3–L5 DRGs (D–F). Scale bar, 30 μm.

Table 2

Electrophysiological characteristics and torque used for normal and noxious rotation for each fibre recorded from rat knee joints

Treatment group	Fibre type	Mechanical threshold (mNm)	Electrical threshold (V)	Conduction velocity ($m \cdot s^{-1}$)	Torque (mNm) Normal rotation	Torque (mNm) Noxious rotation	*n*
2-furoyl-LIGRLO-NH_2	III	16 ± 2	7 ± 2	3.9 ± 1.3	16 ± 1	33 ± 1	6
	IV	19 ± 3	7 ± 1	1.2 ± 0.2	16 ± 1	29 ± 2	11
	ND	13 ± 2	–	–	16 ± 3	22 ± 3	4
SB366791 pre-treated	III	20	5	4.8	13	30	1
	IV	11 ± 3	7 ± 2	1.1 ± 0.2	12 ± 2	21 ± 5	3
	ND	8 ± 1	–	–	11 ± 1	23 ± 3	4
RP67580 + 2-furoyl-LIGRLO-NH_2	III	10 ± 4	5 ± 2	3.3 ± 0.4	15 ± 2	27 ± 2	3
	IV	14 ± 3	7 ± 1	1.2 ± 0.2	14 ± 1	25 ± 4	6
	ND	5	–	–	12 ± 4	23 ± 8	2

Data are mean ± SEM, and fibres are classified as thinly myelinated type III or unmyelinated type IV units. For some fibres, it was not possible to determine conduction velocity. ND, not determined.

Neuronal characteristics of afferent fibres in the rat

Between one and two joint afferent fibres were recorded per rat, with a total of 40 fibres examined overall in the study. Fifty percent of the fibres had conduction velocities that classified them as unmyelinated type IV fibres, whilst 25% were classified as thinly myelinated type III fibres. Conduction velocities could not be determined for 25% of the fibres. No detectable differences were observed in the response of the different groups of afferents to the drugs studied. Table 2 summarizes the electrophysiological characteristics of these

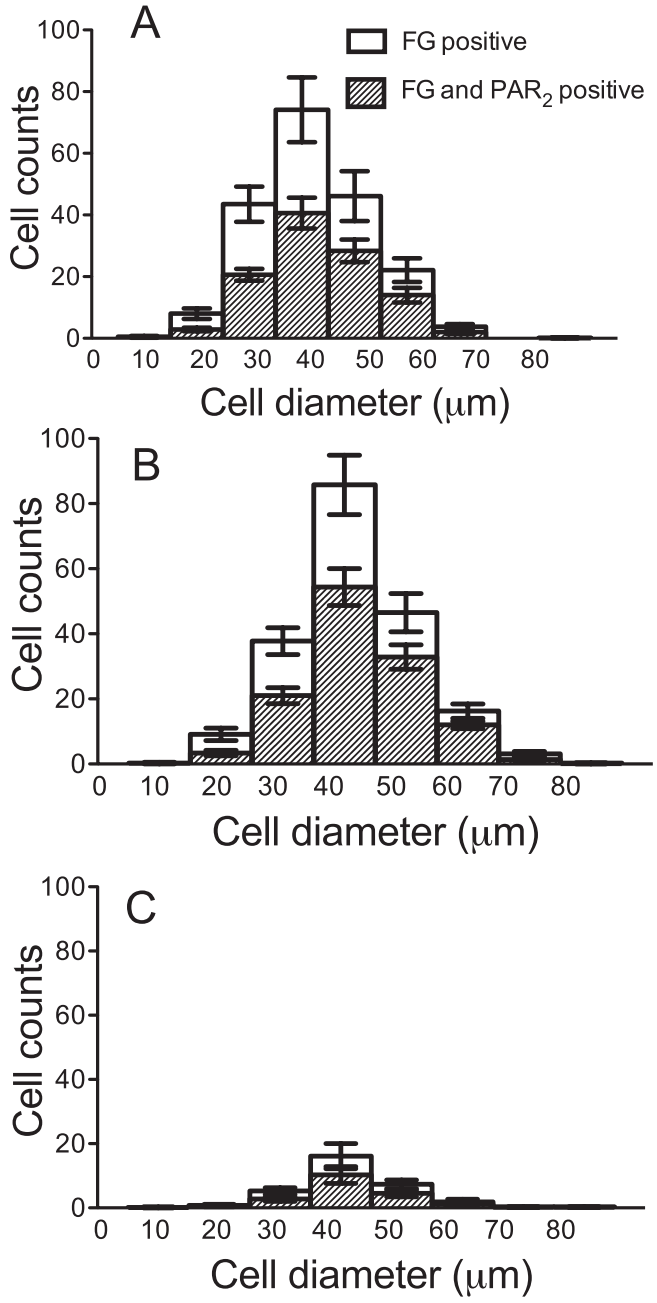

Figure 2

Spread of diameter size neurons positive for Fluoro-Gold (FG) and PAR_2. Diameters of Fluoro-Gold-positive cells in L3 (A), L4 (B) and L5 (C) DRGs. Results are mean ± SEM, $n = 8$.

fibres together with the mean torque levels used for normal and noxious rotation. All fibres tested were responsive to close intra-arterial administration of potassium chloride (KCl; 0.4 mM, 0.1 mL) at the conclusion of the experiment, thus confirming that administered drugs reached the mechanosensory nerve endings. Fibres responded to outward rotation of the knee, and all but one fibre responded to both normal and noxious hyper-rotation of the joint. This single type IV fibre belonging to the 2-furoyl-LIGRLO-NH_2 alone treatment group, only responded to noxious joint rotation. The receptive field of each fibre was identified by gentle probing with a glass rod, and all fell within the area of the knee joint. In contrast to the mouse, little or no spontaneous activity was observed from normal rat knee joint afferent fibres.

Effect of PAR_2 activation on the mechanosensitivity of normal rat knee joint fibres

In the naive rat knee joint, close intra-arterial administration of 100 nmol PAR_2 activating peptide, 2-furoyl-LIGRLO-NH_2 caused a significant increase in joint afferent firing rate from baseline values during both normal and noxious rotation of the joint over 15 min (Figure 4; repeated-measures one-way ANOVA: $P = 0.0002$, normal rotation; $P < 0.0001$, noxious rotation); 10 nmol PAR_2 activating peptide, 2-furoyl-LIGRLO-NH_2 also significantly increased firing rate during noxious rotation but not for the normal movement ($P = 0.09$, normal rotation; $P < 0.0001$, noxious rotation). The lowest dose of 1 nmol 2-furoyl-LIGRLO-NH_2 did not significantly alter firing rate from baseline ($P = 0.76$, normal rotation; $P = 0.30$, noxious rotation). In addition, the control PAR_2-inactive scrambled peptide 2-furoyl-OLGRIL-NH_2, at 100 nmol had no effect on joint fibre firing rate ($P = 0.09$, for both normal and noxious rotations), thus confirming the specificity of 2-furoyl-LIGRLO-NH_2 for activating PAR_2.

The PAR_2 activating peptide had a dose and time-dependent effect on firing rate during both normal and noxious movement (two-way ANOVA: $P < 0.05$; Figure 4C and D). The increase in joint afferent firing rate seen during noxious rotation after administration of 100 nmol 2-furoyl-LIGRLO-NH_2 was significant compared with the same dose of scrambled peptide from 3 to 7 min post administration (Figure 4D; two-way ANOVA followed by Bonferroni post-test: $P < 0.05$). By 9 min, firing rate had returned to baseline values. In a subset of fibres, firing rate was followed up to 2 h post drug administration, but no further increase in firing rate was observed (data not shown). In addition, in two fibres the highest dose of 2-furoyl-LIGRLO-NH_2 was administered for a second time, 15 min after the initial dose; but no effect on firing rate was observed, pointing to a desensitization of the receptor (data not shown).

Effect of SB366791 and RP67580 on PAR_2-induced mechanosensitization of joint fibres

To elucidate the mechanisms behind the PAR_2-induced sensitization of afferent fibres in response to a mechanical stimulus, rats were pre-treated with either the TRPV1 antagonist, SB366791 (500 $\mu g \cdot kg^{-1}$ i.p.) or the NK_1 receptor antagonist, RP67580 (2 nmol co-administered with 2-furoyl-LIGRLO-NH_2). SB366791 was administered systemically, whereas RP67580 was administered locally to the knee joint. Therefore, mean firing rate from four movement cycles was determined pre administration of SB366791 and 30 min post systemic administration. Administration of SB366791 alone had no effect on joint firing rate during both normal and noxious joint rotations (firing rate before SB366791: 11.6 ± 2.2, normal rotation; 52.2 ± 9.8, noxious rotation; firing rate 30 min after SB366791: 10.4 ± 4, normal rotation; 40.2 ± 7.0,

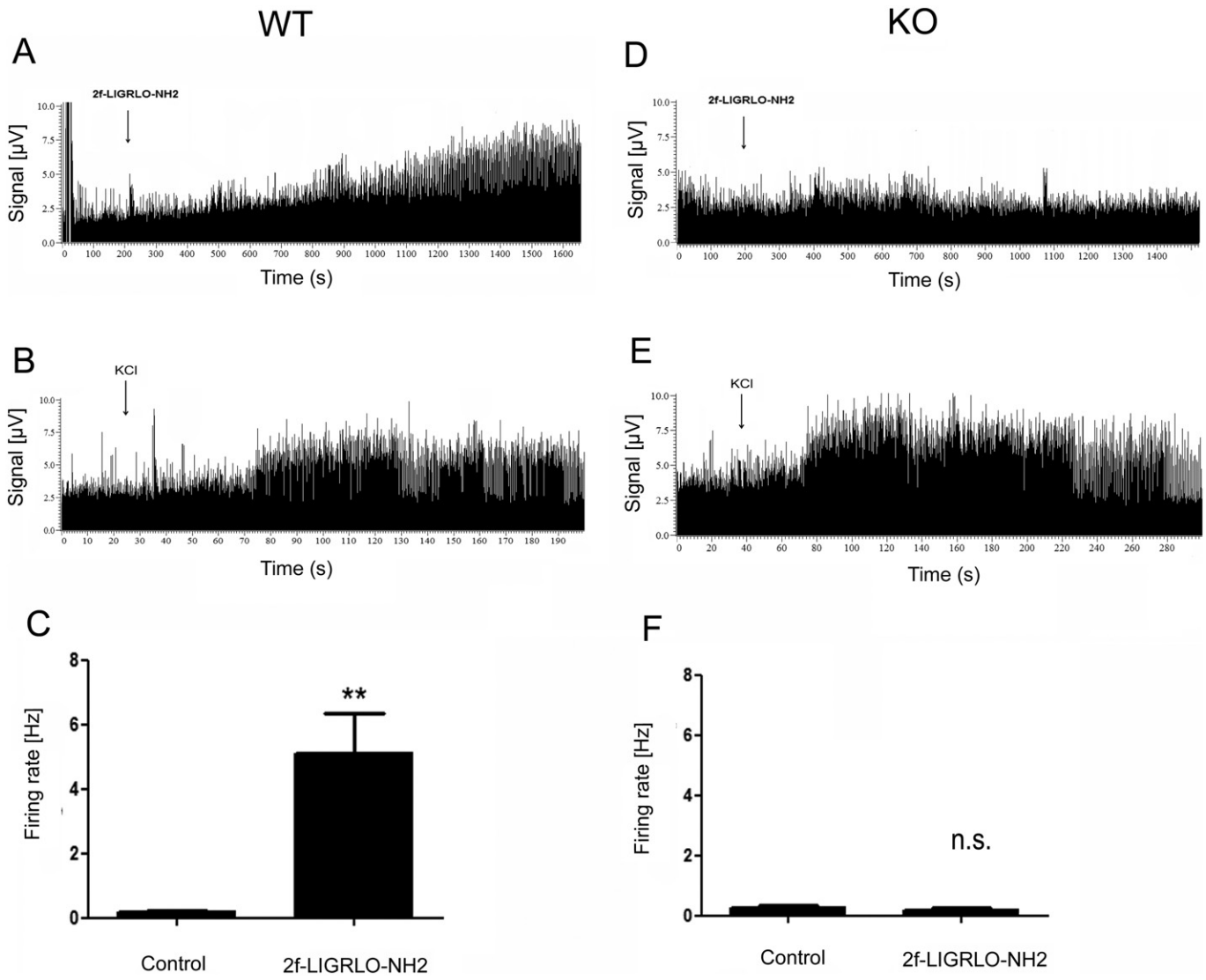

Figure 3

Joint nerve recordings in (A–C) PAR_2 WT and (D–F) PAR_2 KO mice. (A) Example of a multi unit recording from wild-type mouse knee joint afferents. 2-Furoyl-LIGRLO-NH_2 induced long-lasting spontaneous activity in PAR_2 WT mice. (B) KCl was administered subsequently and caused a burst of activity confirming drug exposure to the nerve terminal. (C) The average firing frequency was significantly increased 15 min after 2-furoyl-LIGRLO-NH_2 application in PAR_2 WT mice. Data are shown as mean ± SEM, $n = 6$ animals. Student's *t*-test: ** $P < 0.01$, compared with control. (D) Example of a multi unit recording from knee joint afferents from a PAR_2 KO mouse. 2-Furoyl-LIGRLO-NH_2 had no effect on spontaneous firing in PAR_2 KO mice joint afferents. (E) KCl induced a burst of spontaneous activity in PAR_2 KO mice joint afferents. (F) 2-Furoyl-LIGRLO-NH_2 had no significant effect on average spontaneous firing rate 15 min after drug exposure in PAR_2 KO mice. Data are shown as mean ± SEM, $n = 4$ animals. Student's *t*-test: n.s = not significant compared with control.

noxious rotation; $n = 6$–9). The mean firing rate 30 min after SB366791 was then used as the baseline level in Figure 5A and B. There was no difference between 2-furoyl-LIGRLO-NH_2 alone and after pre-treatment with SB366791 during normal rotation (Figure 5A). However, during noxious joint rotation, pre-treatment with SB366791 completely abolished the increase in firing rate seen with 100 nmol 2-furoyl-LIGRLO-NH_2 (Figure 5B). Interestingly, despite SB366791 alone having no effect on firing rate, when 2-furoyl-LIGRLO-NH_2 was administered after SB366791, the joint firing rate during noxious rotation was significantly reduced from baseline values at 9, 11, 13 and 15 min after administration (Figure 5B, $P < 0.05$; Dunnett's multiple comparison test) during noxious joint rotation.

RP67580 was administered locally via the saphenous artery cannulation; therefore, it was possible to take firing rate measurements for 15 min after RP67580 and before administration of 2-furoyl-LIGRLO-NH_2. These results are shown graphically in Figure 5C and D. Administration of RP67580 alone had no effect on joint firing rate compared with baseline during normal and noxious rotation of the joint (Figure 5C and D). As with SB366791, during normal

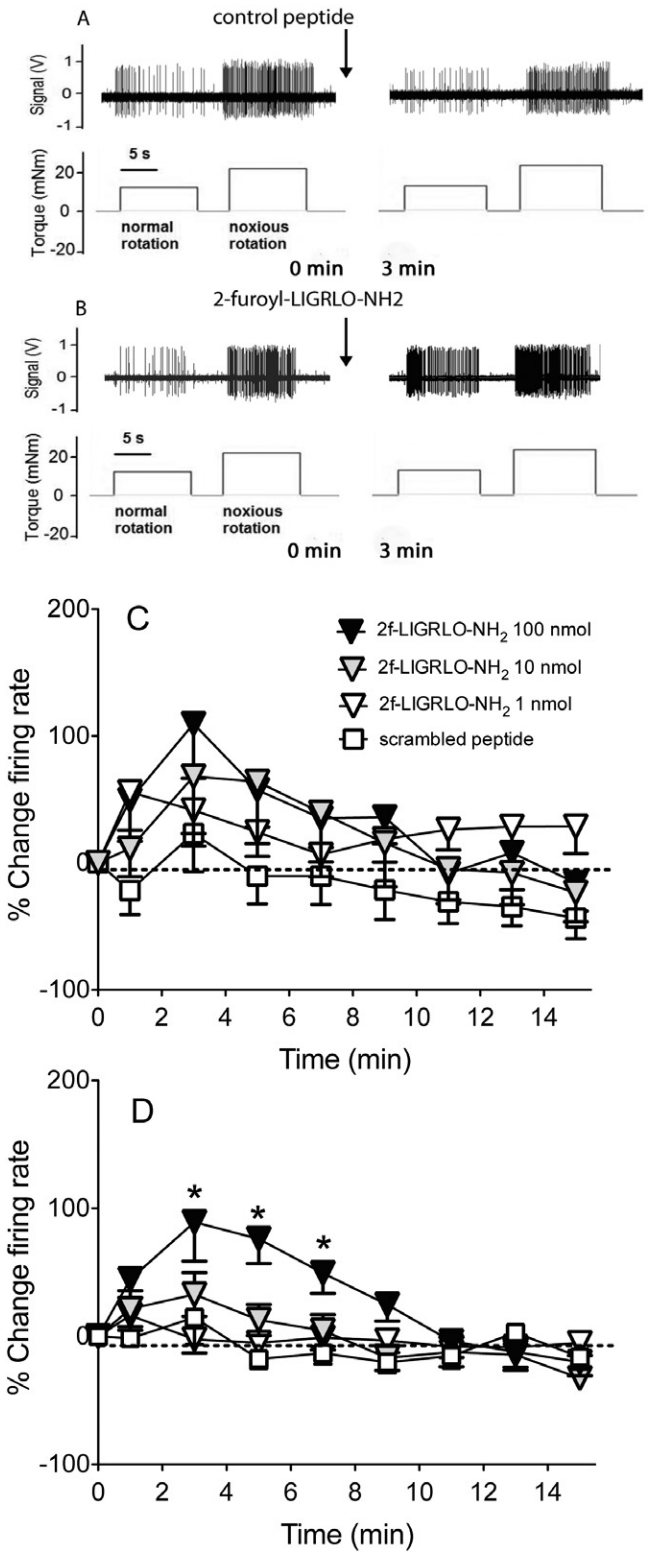

Figure 4

Effect of PAR_2 activation on joint fibre firing in response to a mechanical stimulus. Example of a single unit recording from a single joint fibre before and 3 min after (A) 100 nmol scrambled control peptide 2-furoyl-OLGRIL-NH_2 and (B) 100 nmol 2-furoyl-LIGRLO-NH_2 during normal and noxious rotation of the knee joint. Time course of close intra-arterial injection of either 2-furoyl-LIGRLO-NH_2 (at doses 1–100 nmol·100 μL^{-1}) or scrambled peptide, 2-furoyl-OLGRIL-NH_2 (100 nmol·100 μL^{-1}) on knee joint afferent activity over 15 min in response to (C) normal and (D) noxious rotation of the knee joint. Baseline values before drug administration were used as control. Data are shown as mean ± SEM, $n = 10–21$. Two-way ANOVA followed by Bonferroni test. *$P < 0.05$ compared with scrambled peptide.

rotation, there was no difference in the firing rates between 2-furoyl-LIGRLO-NH_2 alone and 2-furoyl-LIGRLO-NH_2 co-administered with RP67580. However, during noxious rotation RP67580 prevented the increase in firing rate caused by 100 nmol 2-furoyl-LIGRLO-NH_2 (Figure 5D). A similar result was observed as with SB366791, in that a significant decrease in firing rate from baseline values was seen from 11 to 15 min when RP67580 was co-administered with 2-furoyl-LIGRLO-NH_2 (Figure 5D, $P < 0.05$; Dunnett's multiple comparison test).

Effect of PAR_2 activation on leukocyte kinetics in the knee joint

Leukocyte rolling. Perfusion of saline vehicle alone caused a small but significant increase in leukocyte rolling in the microvasculature of the joint over 50 min (Figure 6A, repeated-measures one-way ANOVA; $P < 0.001$). This increase could be due to a small inflammatory effect caused by exposure of the knee joint alone. However, perfusion of all three doses of 2-furoyl-LIGRLO-NH_2 for 5 min caused a heightened increase in leukocyte rolling in the joint (Figure 6A). This increase was significantly enhanced compared with vehicle from 5 min post perfusion and lasted up to 50 min (Figure 6A). There was no difference between the different doses of the PAR_2 peptide perhaps indicating that even at the lowest dose; maximal leukocyte rolling had been induced. In contrast, the scrambled receptor-inactive peptide at a dose equivalent to the highest one used for the receptor-active peptide had no effect on leukocyte rolling compared with vehicle (Figure 6A).

Leukocyte adhesion. Perfusion of saline vehicle alone also caused a significant, albeit minor, increase in leukocyte adhesion in the joint over the 50 min recording period (from 0.4 ± 0.2 adherent leukocytes to 2.6 ± 0.2 at 50 min, Figure 6B; repeated-measures one-way ANOVA; $P < 0.0001$). However, 2-furoyl-LIGRLO-NH_2 enhanced this leukocyte adhesion at all doses (from 1 μM to 1 mM) compared with vehicle. At a concentration of 1 mM, 2-furoyl-LIGRLO-NH_2 caused the number of adherent leukocytes to increase from 0.7 ± 0.3 at baseline, to 9.2 ± 1 at 50 min. As with leukocyte rolling, this effect was observed from 5 min post perfusion and persisted for up to 60 min (Figure 6B). 1 mM 2-furoyl-LIGRLO-NH_2 had a significantly greater maximum effect compared with the two lower doses of the PAR_2 activating peptide, 1 μM and 10 μM. The scrambled PAR_2-inactive peptide at the same concentration as the highest dose of 2-furoyl-LIGRLO-NH_2 (1 mM) had no effect on leukocyte adhesion compared with vehicle (Figure 6B).

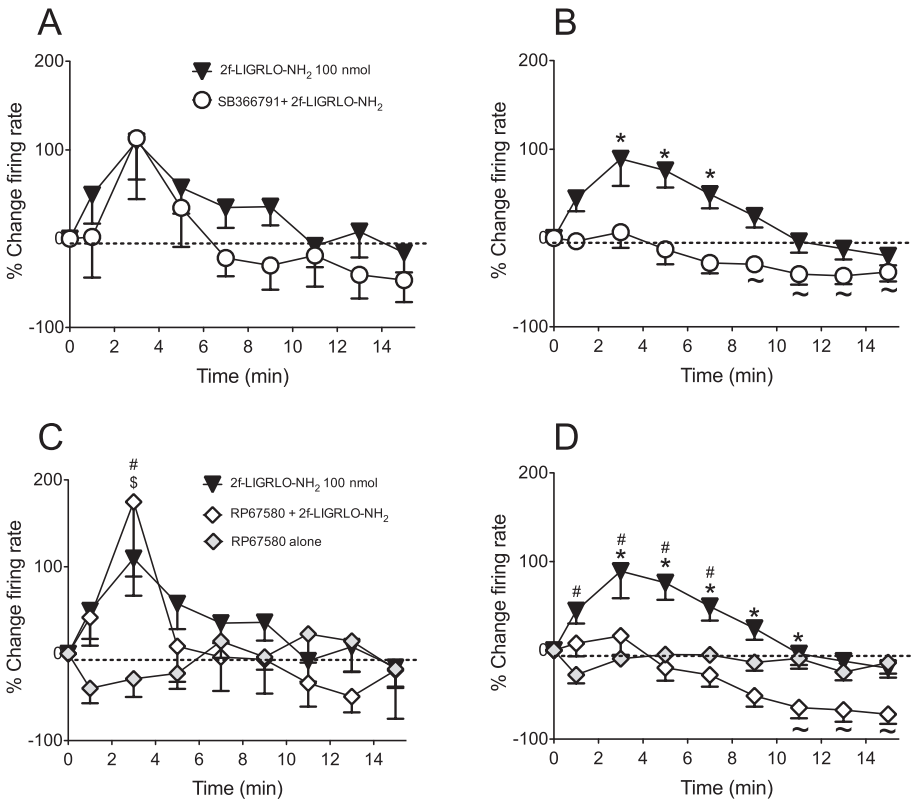

Figure 5

Effect of TRPV1 and NK_1 receptor antagonism on PAR_2-induced sensitization of joint fibres. Time course of knee joint afferent activity over 15 min after close intra-arterial injection of 2-furoyl-LIGRLO-NH_2 (100 nmol·100 μL^{-1}) alone (n = 21) or 30 min after treatment with SB366791 (500 $\mu g \cdot kg^{-1}$ i.p., n = 8) in response to (A) non-noxious and (B) noxious rotation of the joint. Two-way ANOVA followed by Bonferroni test. *$P < 0.05$ compared with SB366791 pre-treated. Repeated-measures one-way ANOVA followed by Dunnet's multiple comparison test to compare against baseline, ~$P < 0.05$. Time course of 2-furoyl-LIGRLO-NH_2 (100 nmol·100 μL^{-1}) alone (n = 21), co-administered with RP67580 (2 nmol, n = 11), or RP67580 alone (n = 8) in response to (C) non-noxious and (D) noxious rotation of the knee joint. Data are shown as mean ± SEM. Two-way ANOVA followed by Bonferroni test. *$P < 0.05$ compared with RP67580 + 2-furoyl-LIGRLO-NH_2, #$P < 0.05$ compared with RP67580 alone, \$$P < 0.05$ RP67580 + 2-furoyl-LIGRLO-NH_2 compared with RP67580 alone. Repeated-measures one-way ANOVA followed by Dunnet's multiple comparison test to compare against baseline, ~$P < 0.05$.

Effect of SB366791 and RP67580 on PAR_2-induced leukocyte rolling and adhesion

Pre-treatment with either SB366791 or RP67580 significantly inhibited the PAR_2-induced increase in leukocyte rolling (Figure 7A) and adhesion (Figure 7B) over the time course of the experiment at all doses of 2-furoyl-LIGRLO-NH_2 tested ($P < 0.05$, repeated-measures two-way ANOVA). The effect at 40 min is illustrated in Figure 7 and shows the ability of either SB366791 or RP67580 to inhibit both rolling and adherence of leukocytes at the 40 min time point. This result is representative of the inhibition observed at all other time points (not shown).

Discussion

The main findings of this study were that PAR_2 receptors were co-localized in neuronal cell bodies receiving afferent projections from the knee joint,and that PAR_2 activation did affect both afferent activity and leukocyte trafficking in the knee joint. The knowledge that serine proteinases are seen in high levels in chronic joint disease and have the ability to signal through the PAR family of receptors, has led to intensive research on the effect of PAR activation in the joint. In this study, we have advanced the understanding of the role of PAR_2 in the rat knee joint. We have shown for the first time, that PAR_2 receptors are highly expressed in joint sensory neurones and that activation of these receptors led to a transient sensitization of these joint fibres, together with a sustained increase in leukocyte rolling and adhesion in the microvasculature of the joint. Despite the fact that, in other tissues, there is no correlation between the leukocyte trafficking and neuronal effects of PAR_2 activation, we have shown here that both of the effects on leukocyte kinetics and the neuronal sensitization caused by PAR_2 in the joint appear to be mediated via TRPV1 and NK_1 receptors.

Previously, we have shown that activation of the another member of the PAR family, PAR_4, sensitizes knee joint afferent fibres with a significant increase in firing rate observed from 1 min and sustained over 15 min during both normal and noxious joint rotations (Russell *et al.*, 2010). In contrast,

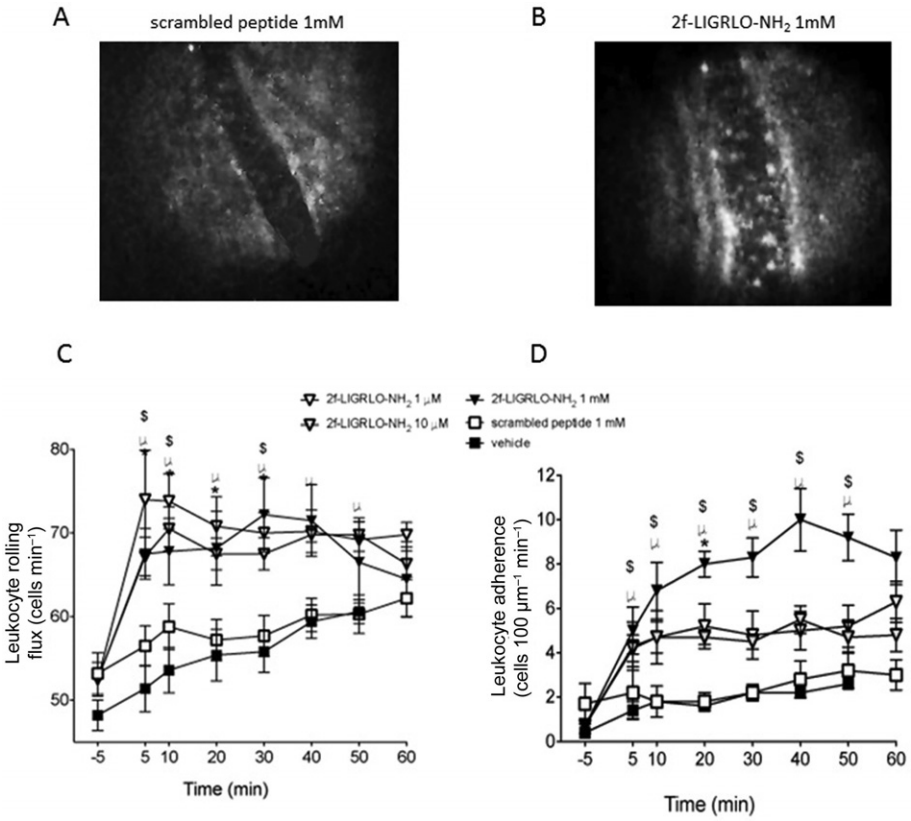

Figure 6

Effect of PAR_2 activation on leukocyte kinetics. Representative intravital microscope images showing the lack of effect of the scrambled peptide (A) and the stimulatory effect of 2-furoyl-LIGRLO-NH_2 (B) on leukocyte accumulation in a joint blood vessel. Time course of (C) leukocyte rolling and (D) leukocyte adhesion after perfusion of 2-furoyl-LIGRLO-NH_2 (doses 1–1000 μM) or scrambled peptide, 2-furoyl-OLGRIL-NH_2 (1000 μM) over 60 min. Data are shown as mean ± SEM, n = 5–6. Two-way ANOVA followed by Bonferroni test. *P < 0.05 1 μM 2-furoyl-LIGRLO-NH_2, #P < 0.05 10 μM 2-furoyl-LIGRLO-NH_2, $$P$ < 0.05 1000 μM 2-furoyl-LIGRLO-NH_2 compared with vehicle. ∞P < 0.05 1000 μM 2-furoyl-LIGRLO-NH_2 compared with 1000 μM 2-furoyl-OLGRIL-NH_2.

activation of PAR_2, examined in this new study, caused a transient sensitization of joint afferents during both normal and noxious rotations (Figure 4C and D). The increased firing rate during noxious rotation does not become significant from control peptide until 3 min post administration and only lasts for 7 min. Both PAR_4 and PAR_2 receptors were expressed in similar proportions and with a similar neuronal size distribution in the DRG neurones from fibres innervating the joint (Russell *et al.*, 2010). Despite this similarity in receptor distribution, PAR_2 and PAR_4 receptors work via different mechanisms. PAR_4-induced sensitization was reported to be TRPV1-independent but dependent on both the bradykinin B_2 receptor and connective tissue mast cells (Russell *et al.*, 2010; 2011). Conversely, PAR_2-induced sensitization in the context of a noxious stimulus is both TRPV1 and NK_1 receptor-dependent (Figure 5B and D). Due to the transient nature of this sensitization, it may be hypothesized that 2-furoyl-LIGRLO-NH_2 is working directly on PAR_2 receptors expressed on the peripheral terminals of the afferent fibres, rather than activating other cell types, such as mast cells as was observed in the PAR_4 study. Once activated, PAR_2 receptors are rapidly desensitised, followed by internalization and degradation (Bohm *et al.*, 1996; Adams *et al.*, 2011). This desensitization process accounts for the lack of effect we observed when a second dose of 100 nmol 2-furoyl-LIGRLO-NH_2, was administered 15 min after the initial dose. Resensitization of PAR_2 receptors is thought to take between 30 and 60 min after desensitization and occurs by both mobilization of intracellular pools of these receptors to the plasma membrane and *de novo* receptor synthesis (Bohm *et al.*, 1996).

Antagonism of either TRPV1 or NK_1 receptors prevented PAR_2-induced neuronal sensitization, but only during noxious joint rotation. These findings corroborate a previous study that showed that intra-articular injection of a PAR_2 agonist caused a painful response in the rat hind limb via a TRPV1-dependent pathway (Helyes *et al.*, 2010). PAR_2 receptors have been previously shown to sensitise TRPV1 channels via PKA, PKC and PLC-dependent pathways (Amadesi *et al.*, 2004; 2006; Dai *et al.*, 2004), thus lowering their activation threshold. The current data show that this effect occurs only during noxious joint rotation indicating that TRPV1 channels were only activated by suprathreshold stimuli in non-inflamed tissue. The role for TRPV1 channels in mechanosensation is controversial with $TRPV1^{-/-}$ mice exhibiting no difference in sensitivity to mechanical stimuli (Caterina *et al.*, 2000; Davis *et al.*, 2000). More recently, however, results with TRPV1

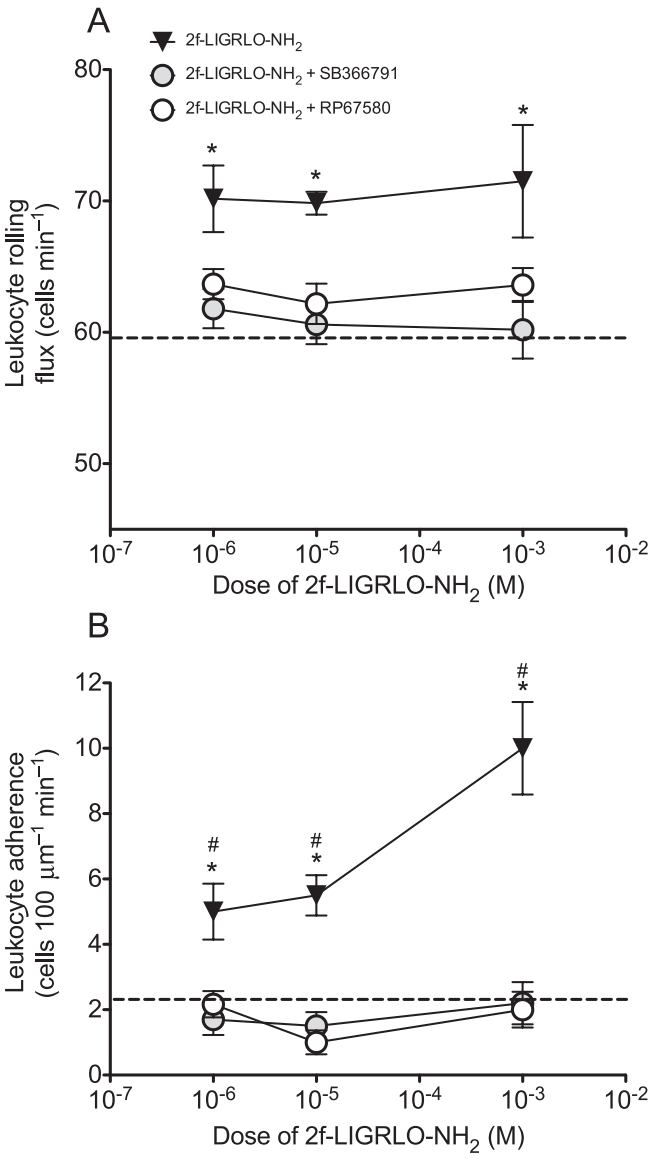

Figure 7

Effect of TRPV1 and NK_1 receptor antagonism on PAR_2-induced changes in leukocyte kinetics. Dose–response of (A) leukocyte rolling and (B) leukocyte adhesion 40 min after perfusion of 2-furoyl-LIGRLO-NH_2 (doses 1–1000 μM). Rats were either naive or pre-treated with SB366791 (500 $\mu g \cdot kg^{-1}$ i.p. 30 min before perfusion) or RP67580 (200 μM) was co-perfused with 2-furoyl-LIGRLO-NH_2. Data are shown as mean ± SEM, n = 5–10. Two-way ANOVA followed by Bonferroni test. *P < 0.05 compared with SB366791 pre-treated, #P < 0.05 compared with RP67580 treated. Dotted line is equivalent to value after perfusion of vehicle at 40 min.

channel antagonists have suggested a role for these receptors in mechanical allodynia (Kanai *et al.*, 2005; Cui *et al.*, 2006; Fernandes *et al.*, 2011). Thus, TRPV1 channels may play a more important role detecting noxious mechanical stimuli compared with a normal mechanical stimulus. Other members of the TRP channel family, namely TRPV4, TRPA1, and TRPM8 have all been implicated in mechanosensation (Grant *et al.*, 2007; Brierley *et al.*, 2011; Fernandes *et al.*, 2011; Harrington *et al.*, 2011) and significantly, links between PAR_2 receptors have been observed with both TRPA1 and TRPV4 channels (Dai *et al.*, 2007; Grant *et al.*, 2007). Therefore, during normal rotation, PAR_2 receptors could be mediating their sensitizing effects via TRPA1 or TRPV4 channels, but this possibility requires further investigation.

The substance P receptor, NK_1 is also required for the PAR_2-induced sensitization during noxious rotation, implying a role for the sensory neuropeptide, substance P, in sensitizing the joint afferents. Activation of TRPV1 channels leads to substance P release from the peripheral terminals of sensory nerves, where it can work in an autocrine and/or paracrine fashion activating NK_1 receptors expressed both on these peripheral terminals and on adjacent parenchymal cells (Zhang *et al.*, 2007). This action can thus contribute to peripheral sensitization (Richardson and Vasko, 2002). This suggestion is in keeping with previous studies showing that the NK_1 receptor is crucial for the hyperalgesia caused by injection of PAR_2 activating peptides into the hind paw of rodents (Vergnolle *et al.*, 2001) Interestingly, in our new work described here, antagonism of TRPV1 and NK_1 receptors together with administration of the PAR_2 activating peptide in the context of noxious rotation, causes a significant reduction in afferent fibre firing rate below that of baseline beginning at about 9 min after administration of 2-furoyl-LIGRLO-NH_2 (Figure 5B and D). This decrease was not observed after treatment with the antagonists alone, presumably because without concurrent PAR_2 receptor stimulation, the activation threshold of TRPV1 channels was not lowered. Hence, in that situation, the noxious rotation may not be sufficient to activate TRPV1 channels, and therefore, no substance P is released. The reduced firing rate observed with the antagonists in the course of PAR_2 activation, may be due to PAR_2 receptors causing the release of analgesic mediators such as cannabinoids or opioids from either neuronal or non-neuronal sources; such agonists are known to be anti-nociceptive in the joint (Li *et al.*, 2005; Schuelert and McDougall, 2008; McDougall, 2011). This 'analgesic' effect of PAR_2 activation may normally be masked by the predominant pro-algesic effect of TRPV1 activation and substance P release.

Our work is the first to show that PAR_2 activation causes increased leukocyte rolling and adhesion in the microvasculature of the joint. This finding correlates with findings (i) in the cremaster muscle of mice where treatment with the PAR_2 peptide, SLIGRL-NH_2 induces P-selectin expression on endothelial cells, thus enhancing leukocyte rolling (Lindner *et al.*, 2000), and (ii) in the paw, where PAR_2 activation results in leukocyte accumulation (Vergnolle *et al.*, 1999). As with the PAR_2-induced neuronal sensitization, the PAR_2-induced changes in leukocyte kinetics were observed to be dependent on TRPV1 and NK_1 receptors. It is well known that substance P, released after TRPV1 activation, acts on the NK_1 receptor and is a potent mediator of increased microvascular permeability (Cao *et al.*, 2000). In addition, substance P can enhance the expression of P-selectin on endothelial cells thus promoting leukocyte rolling and tethering as well as potentiating leukocyte accumulation during inflammation over a number of hours (Cao *et al.*, 2000; Miyazaki *et al.*, 2006). The microvascular effects of substance P can be prevented by prior neuronal desensitization with capsaicin and pre-treatment with TRPV1 antagonists (Richardson and Vasko, 2002; Varga

et al., 2005), implicating an important role for neuronal TRPV1 channels in this process.

PAR_2 expression was observed in approximately 60% of knee joint afferents, but it is still not known whether the PAR_2 activating peptide is acting directly on neuronal PAR_2 receptors in our model. PAR_2 receptors are also expressed in endothelial cells and various immune cells, such as macrophages, neutrophils and mast cells (Russell and McDougall, 2009). However, we have shown here that activation of TRPV1 and NK_1 receptors are crucial in mediating both the neuronal sensitization and increased leukocyte rolling and adhesion induced by PAR_2 activation in the joint. It is essential to learn more about the role of PAR_2 in the joint, as this receptor is emerging as a key player in chronic inflammatory joint disease (Ferrell *et al.*, 2003; 2010; Yang *et al.*, 2005; Kelso *et al.*, 2006; Busso *et al.*, 2007; Nakano *et al.*, 2007). Problems with the development of selective PAR_2 antagonists have hindered the clinical translation of these findings. Thus, greater knowledge of the pathways involved in PAR_2-mediated effects in the joint, may allow for the development of improved therapies to deal with the widespread clinical problem of chronic joint pain and inflammation.

Acknowledgements

This work was supported by operating grants from the Canadian Institutes for Health Research (to JJMcD and MDH) and an equipment/infrastructure grant from the Canadian Foundation for Innovation (CFI) and the Alberta Science and Research Authority. JJMcD holds a Senior Scholar award from the Alberta Heritage Foundation for Medical Research (AHFMR) and an Investigator award from the Arthritis Society of Canada. FAR and NS receive postdoctoral support from AHFMR and the Canadian Arthritis Network.

Conflicts of interest

There are no conflicts.

References

Adams MN, Ramachandran R, Yau MK, Suen JY, Fairlie DP, Hollenberg MD *et al.* (2011). Structure, function and pathophysiology of protease activated receptors. Pharmacol Ther 130: 248–282.

Al-Ani B, Saifeddine M, Kawabata A, Renaux B, Mokashi S, Hollenberg MD (1999). Proteinase-activated receptor 2 (PAR(2)): development of a ligand-binding assay correlating with activation of PAR(2) by PAR(1)- and PAR(2)-derived peptide ligands. J Pharmacol Exp Ther 290: 753–760.

Alexander SPH, Mathie A, Peters JA (2011). Guide to Receptors and Channels (GRAC), 5th edn. Br J Pharmacol 164 (Suppl. 1): S1–S324.

Alier KA, Endicott JA, Stemkowski PL, Cenac N, Cellars L, Chapman K *et al.* (2008). Intrathecal administration of proteinase-activated receptor-2 agonists produces hyperalgesia by exciting the cell bodies of primary sensory neurons. J Pharmacol Exp Ther 324: 224–233.

Amadesi S, Nie J, Vergnolle N, Cottrell GS, Grady EF, Trevisani M *et al.* (2004). Protease-activated receptor 2 sensitizes the capsaicin receptor transient receptor potential vanilloid receptor 1 to induce hyperalgesia. J Neurosci 24: 4300–4312.

Amadesi S, Cottrell GS, Divino L, Chapman K, Grady EF, Bautista F *et al.* (2006). Protease-activated receptor 2 sensitizes TRPV1 by protein kinase Cepsilon- and A-dependent mechanisms in rats and mice. J Physiol 575: 555–571.

Andruski B, McCafferty DM, Ignacy T, Millen B, McDougall JJ (2008). Leukocyte trafficking and pain behavioral responses to a hydrogen sulfide donor in acute monoarthritis. Am J Physiol Regul Integr Comp Physiol 295: R814–R820.

Bohm SK, Khitin LM, Grady EF, Aponte G, Payan DG, Bunnett NW (1996). Mechanisms of desensitization and resensitization of proteinase-activated receptor-2. J Biol Chem 271: 22003–22016.

Brierley SM, Castro J, Harrington AM, Hughes PA, Page AJ, Rychkov GY *et al.* (2011). TRPA1 contributes to specific mechanically activated currents and sensory neuron mechanical hypersensitivity. J Physiol 589: 3575–3593.

Busso N, Frasnelli M, Feifel R, Cenni B, Steinhoff M, Hamilton J *et al.* (2007). Evaluation of protease-activated receptor 2 in murine models of arthritis. Arthritis Rheum 56: 101–107.

Cao T, Pinter E, Al Rashed S, Gerard N, Hoult JR, Brain SD (2000). Neurokinin-1 receptor agonists are involved in mediating neutrophil accumulation in the inflamed, but not normal, cutaneous microvasculature: an *in vivo* study using neurokinin-1 receptor knockout mice. J Immunol 164: 5424–5429.

Caterina MJ, Leffler A, Malmberg AB, Martin WJ, Trafton J, Petersen-Zeitz KR *et al.* (2000). Impaired nociception and pain sensation in mice lacking the capsaicin receptor. Science 288: 306–313.

Coelho AM, Vergnolle N, Guiard B, Fioramonti J, Bueno L (2002). Proteinases and proteinase-activated receptor 2: a possible role to promote visceral hyperalgesia in rats. Gastroenterology 122: 1035–1047.

Costa R, Marotta DM, Manjavachi MN, Fernandes ES, Lima-Garcia JF, Paszcuk AF *et al.* (2008). Evidence for the role of neurogenic inflammation components in trypsin-elicited scratching behaviour in mice. Br J Pharmacol 154: 1094–1103.

Cui M, Honore P, Zhong C, Gauvin D, Mikusa J, Hernandez G *et al.* (2006). TRPV1 receptors in the CNS play a key role in broad-spectrum analgesia of TRPV1 antagonists. J Neurosci 26: 9385–9393.

Dai Y, Moriyama T, Higashi T, Togashi K, Kobayashi K, Yamanaka H *et al.* (2004). Proteinase-activated receptor 2-mediated potentiation of transient receptor potential vanilloid subfamily 1 activity reveals a mechanism for proteinase-induced inflammatory pain. J Neurosci 24: 4293–4299.

Dai Y, Wang S, Tominaga M, Yamamoto S, Fukuoka T, Higashi T *et al.* (2007). Sensitization of TRPA1 by PAR2 contributes to the sensation of inflammatory pain. J Clin Invest 117: 1979–1987.

Damiano BP, Cheung WM, Santulli RJ, Fung-Leung WP, Ngo K, Ye RD *et al.* (1999). Cardiovascular responses mediated by protease-activated receptor-2 (PAR-2) and thrombin receptor (PAR-1) are distinguished in mice deficient in PAR-2 or PAR-1. J Pharmacol Exp Ther 288: 671–678.

Davis JB, Gray J, Gunthorpe MJ, Hatcher JP, Davey PT, Overend P *et al.* (2000). Vanilloid receptor-1 is essential for inflammatory thermal hyperalgesia. Nature 405: 183–187.

Fernandes ES, Russell FA, Spina D, McDougall JJ, Graepel R, Gentry C *et al.* (2011). A distinct role for TRPA1, in addition to

TRPV1, in TNFalpha-induced inflammatory hyperalgesia and CFA-induced mono-arthritis. Arthritis Rheum 63: 819–829.

Ferrell WR, Lockhart JC, Kelso EB, Dunning L, Plevin R, Meek SE *et al.* (2003). Essential role for proteinase-activated receptor-2 in arthritis. J Clin Invest 111: 35–41.

Ferrell WR, Kelso EB, Lockhart JC, Plevin R, McInnes IB (2010). Protease-activated receptor 2: a novel pathogenic pathway in a murine model of osteoarthritis. Ann Rheum Dis 69: 2051–2054.

Grant AD, Cottrell GS, Amadesi S, Trevisani M, Nicoletti P, Materazzi S *et al.* (2007). Protease-activated receptor 2 sensitizes the transient receptor potential vanilloid 4 ion channel to cause mechanical hyperalgesia in mice. J Physiol 578: 715–733.

Hansen KK, Sherman PM, Cellars L, Andrade-Gordon P, Pan Z, Baruch A *et al.* (2005). A major role for proteolytic activity and proteinase-activated receptor-2 in the pathogenesis of infectious colitis. Proc Natl Acad Sci USA 102: 8363–8368.

Harrington AM, Hughes PA, Martin CM, Yang J, Castro J, Isaacs NJ *et al.* (2011). A novel role for TRPM8 in visceral afferent function. Pain 152: 1459–1468.

Helyes Z, Sandor K, Borbely E, Tekus V, Pinter E, Elekes K *et al.* (2010). Involvement of transient receptor potential vanilloid 1 receptors in protease-activated receptor-2-induced joint inflammation and nociception. Eur J Pain 14: 351–358.

Hollenberg MD, Compton SJ (2002). International Union of Pharmacology. XXVIII. Proteinase-activated receptors. Pharmacol Rev 54: 203–217.

Hollenberg MD, Renaux B, Hyun E, Houle S, Vergnolle N, Saifeddine M *et al.* (2008). Derivatized 2-furoyl-LIGRLO-amide, a versatile and selective probe for proteinase-activated receptor 2: binding and visualization. J Pharmacol Exp Ther 326: 453–462.

Ivanavicius SP, Blake DR, Chessell IP, Mapp PI (2004). Isolectin B4 binding neurons are not present in the rat knee joint. Neuroscience 128: 555–560.

Kanai Y, Nakazato E, Fujiuchi A, Hara T, Imai A (2005). Involvement of an increased spinal TRPV1 sensitization through its up-regulation in mechanical allodynia of CCI rats. Neuropharmacology 49: 977–984.

Kawabata A, Kawao N, Kuroda R, Tanaka A, Itoh H, Nishikawa H (2001). Peripheral PAR-2 triggers thermal hyperalgesia and nociceptive responses in rats. Neuroreport 12: 715–719.

Kawabata A, Kanke T, Yonezawa D, Ishiki T, Saka M, Kabeya M *et al.* (2004). Potent and metabolically stable agonists for protease-activated receptor-2: evaluation of activity in multiple assay systems *in vitro* and *in vivo*. J Pharmacol Exp Ther 309: 1098–1107.

Kelso EB, Lockhart JC, Hembrough T, Dunning L, Plevin R, Hollenberg MD *et al.* (2006). Therapeutic promise of proteinase-activated receptor-2 antagonism in joint inflammation. J Pharmacol Exp Ther 316: 1017–1024.

Li Z, Proud D, Zhang C, Wiehler S, McDougall JJ (2005). Chronic arthritis down-regulates peripheral mu-opioid receptor expression with concomitant loss of endomorphin 1 antinociception. Arthritis Rheum 52: 3210–3219.

Lindner JR, Kahn ML, Coughlin SR, Sambrano GR, Schauble E, Bernstein D *et al.* (2000). Delayed onset of inflammation in protease-activated receptor-2-deficient mice. J Immunol 165: 6504–6510.

McDougall JJ (2011). Peripheral analgesia: hitting pain where it hurts. Biochim Biophys Acta 1812: 459–467.

McDougall JJ, Hanesch U, Pawlak M, Schmidt RF (2001). Participation of NK1 receptors in nociceptin-induced modulation of rat knee joint mechanosensitivity. Exp Brain Res 137: 249–253.

McGrath J, Drummond G, Kilkenny C, Wainwright C (2010). Guidelines for reportingexperiments involving animals: the ARRIVE guidelines. Br J Pharmacol 160: 1573–1576.

Macfarlane SR, Seatter MJ, Kanke T, Hunter GD, Plevin R (2001). Proteinase-activated receptors. Pharmacol Rev 53: 245–282.

Miyazaki Y, Satoh T, Nishioka K, Yokozeki H (2006). STAT-6-mediated control of P-selectin by substance P and interleukin-4 in human dermal endothelial cells. Am J Pathol 169: 697–707.

Nakano S, Mishiro T, Takahara S, Yokoi H, Hamada D, Yukata K *et al.* (2007). Distinct expression of mast cell tryptase and protease activated receptor-2 in synovia of rheumatoid arthritis and osteoarthritis. Clin Rheumatol 26: 1284–1292.

Oikonomopoulou K, Hansen KK, Saifeddine M, Tea I, Blaber M, Blaber SI *et al.* (2006). Proteinase-activated receptors, targets for kallikrein signaling. J Biol Chem 281: 32095–32112.

Ramachandran R, Hollenberg MD (2008). Proteinases and signalling: pathophysiological and therapeutic implications via PARs and more. Br J Pharmacol 153 (Suppl. 1): S263–S282.

Richardson JD, Vasko MR (2002). Cellular mechanisms of neurogenic inflammation. J Pharmacol Exp Ther 302: 839–845.

Russell FA, McDougall JJ (2009). Proteinase activated receptor (PAR) involvement in mediating arthritis pain and inflammation. Inflamm Res 58: 119–126.

Russell FA, Veldhoen VE, Tchitchkan D, McDougall JJ (2010). Proteinase-activated receptor-4 (PAR4) activation leads to sensitization of rat joint primary afferents via a bradykinin B2 receptor-dependent mechanism. J Neurophysiol 103: 155–163.

Russell FA, Zhan S, Dumas A, Lagarde S, Pouliot M, McDougall JJ (2011). The pronociceptive effect of proteinase-activated receptor-4 stimulation in rat knee joints is dependent on mast cell activation. Pain 152: 354–360.

Salo PT, Theriault E (1997). Number, distribution and neuropeptide content of rat knee joint afferents. J Anat 190: 515–522.

Schuelert N, McDougall JJ (2008). Cannabinoid-mediated antinociception is enhanced in rat osteoarthritic knees. Arthritis Rheum 58: 145–153.

Steinhoff M, Vergnolle N, Young SH, Tognetto M, Amadesi S, Ennes HS *et al.* (2000). Agonists of proteinase-activated receptor 2 induce inflammation by a neurogenic mechanism. Nat Med 6: 151–158.

Varga A, Nemeth J, Szabo A, McDougall JJ, Zhang C, Elekes K *et al.* (2005). Effects of the novel TRPV1 receptor antagonist SB366791 *in vitro* and *in vivo* in the rat. Neurosci Lett 385: 137–142.

Vergnolle N, Hollenberg MD, Sharkey KA, Wallace JL (1999). Characterization of the inflammatory response to proteinase-activated receptor-2 (PAR2)-activating peptides in the rat paw. Br J Pharmacol 127: 1083–1090.

Vergnolle N, Bunnett NW, Sharkey KA, Brussee V, Compton SJ, Grady EF *et al.* (2001). Proteinase-activated receptor-2 and hyperalgesia: a novel pain pathway. Nat Med 7: 821–826.

Yang YH, Hall P, Little CB, Fosang AJ, Milenkovski G, Santos L *et al.* (2005). Reduction of arthritis severity in protease-activated receptor-deficient mice. Arthritis Rheum 52: 1325–1332.

Zhang H, Cang CL, Kawasaki Y, Liang LL, Zhang YQ, Ji RR, *et al.* (2007). Neurokinin-1 receptor enhances TRPV1 activity in primary sensory neurons via PKCepsilon: a novel pathway for heathyperalgesia. J Neurosci 27: 12067–12077.